Gravitational phase transitions in a one-dimensional spherical system

V. Paige Youngkins and Bruce N. Miller
Department of Physics and Astronomy, Texas Christian University, Fort Worth, Texas 76129
(Received 5 May 2000)

The behavior of gravitational phase transitions in a system of concentric, spherical, mass shells that interact via their mutual and self gravitation is investigated. The nature of the transition in the microcanonical, canonical, and grand canonical ensembles is studied both theoretically in terms of the mean field limit and by dynamical simulation. Transitions between a quasiuniform state and a centrally concentrated state are predicted by mean field theory for the microcanonical and canonical ensembles, and this is supported by dynamical simulation. For the grand canonical ensemble, mean field theory predicts that no transition takes place, and that the thermodynamically stable state is always the uniform one. Again, this is supported by simulations under various initial distributions of mass, even when the system is initialized in a collapsed state. In addition to testing the predictions of the mean field theory and studying the effects of finite size scaling, dynamical simulation allowed us to examine the behavior of temporal and positional correlations which are predicted to vanish in the mean field limit.

PACS number(s): 45.05.+x

I. INTRODUCTION

The focus of this study is the behavior of phase transitions in gravitational systems. Gravitational phase transitions are characterized by a change in the distribution of mass of the system, and have relevance in astrophysical phenomena, such as black hole and planet formation [1,2]. Over the past several decades fundamental questions have been studied concerning the existence and properties of gravitational phase transitions: Are phase transitions possible for gravitating systems? How do they differ from those in ''normal'' matter? How are they influenced by interactions with the environment?

Obtaining answers to these questions is difficult because of the twofold complexity arising from the infinite range and singularity of the gravitational force. In ''normal'' matter studied in laboratory systems, the forces between particles are of short range and, hence, the energy is an extensive parameter. This is not the case in gravitating systems, and a standard thermodynamic analysis can prove intractable. As an approximation, the gravitating system can be considered in the Vlasov (or mean field) limit of an infinite number of particles, $N\rightarrow\infty$, while holding the total mass and energy constant. The system dynamics are represented as a fluid flow in $\mu(\mathbf{r},\boldsymbol{\nu})$ space, and is governed by the collisionless Boltzmann equation (CBE) [3]. For dynamical equilibrium, in which the distribution of the mass does not change with time, the time-independent CBE has an infinite number of stationary solutions. One class of such solutions is polytropes, in which the density as a function of radius is proportional to the nth power of the potential energy of the system [3]. In 1911, Plummer [4] showed that a polytrope of index $n=5$ showed a reasonably good fit to the observational data of some globular clusters. A few years earlier, Emden [5] showed that the special case of infinite polytropic index leads to a *thermal* equilibrium solution, which maximized the entropy for the system. This solution had its own set of difficulties; it does not have a finite radius and has infinite mass.

This situation was stagnant until the 1960s, when Antonov [6] studied the effects of limiting the radius of the system by a reflecting spherical box and determined that the system lacks a global (and for low enough energy a local) entropy maximum. This leads to an instability in which the system may undergo a spontaneous collapse. Lynden-Bell and Wood [7], who referred to this instability as the ''gravothermal catastrophe,'' studied a system of point particles contained in a spherical box, interacting only through their gravitational attraction. They found that for a system with a negative total energy, if the radius of the box was restricted below a critical value, the system possessed a local (but not global) entropy maximum. Local entropy maxima may give rise to long-lived metastable states, but no thermal equilibrium state exists without a global maximum. Lynden-Bell and Wood found that if the radius of the box was above the critical value, there was no local entropy maximum, and a central core existed that would grow hotter and more dense without bound. Later, Hertel and Thirring [8] investigated a system of point fermions interacting by means of their mutual gravitation, and found that, unlike Lynden-Bell and Wood's classical particle system, a global entropy maximum, a true equilibrium state, always exists. This suggested that when the singularity at the origin of the system was shielded, the gravothermal catastrophe was avoided. Aronsen and Hansen [9] shielded the singularity by considering a system of gravitating hard spheres in the mean field limit, and found that the gravothermal catastrophe was replaced by a phase transition from a uniform state to a state with a highly concentrated core. Stahl, Kiessling, and Schindler [2] recently studied a similar hard sphere system for both isoenergetic and isothermal conditions, and found that phase transitions occur in both systems.

In related work, Kiessling [10] investigated the complete N-body gravitating system in the canonical ensemble. He softened the potential, and studied the limit of the partition function as the softening is removed. He proved rigorously that a three-dimensional, nonrelativistic, isothermal system will collapse to a δ-function density distribution. He also proved that a phase transition is possible in the isoenergetic

 ©2000 The American Physical Society

system restricted to a spherical box, if the singularity of the two-body interaction potential is regularized so that it remains bounded at $r=0$.

Until now, none of these thermodynamic predictions of a phase transition was confirmed by studying the dynamical evolution of a gravitational system. Simulation of realistic gravitating systems, such as globular clusters or galaxies, comes with its own set of problems. The singularity in the gravitational force law, escape of stars from the system, binary formation, and stellar evolution complicate the dynamics greatly [3]. Even when stellar evolution is ignored and each star is represented by a simple mass point in three-dimensional space, the amount of computing time required to integrate the system's equations of motion for many relaxation times is considerable. Recent advances in computing hardware, such as the GRAPE family of dedicated computers [11], are making it possible to study large-scale realistic gravitating systems, such as interacting galaxies, with greater precision. As another alternative, idealized models are created that make simulation feasible, while capturing a basic property of the interaction. The ease of computation for one-dimensional systems has made them a popular choice for studying long term behavior. Typically, these models fall into one of two classes: (1) a system of parallel mass sheets [12–16], which has been suggested to have some similarities with the motion of stars perpendicular to the plane of a highly flattened galaxy [17]; and (2) a system of concentric, spherical mass shells, which are identified with the dynamics of a spherical globular cluster [18–21]. Simulations show that if the parallel mass sheet system reaches equilibrium at all, it takes a very long time. This casts into question its usefulness as a test model, and has stimulated a search for other systems which unambiguously relax to equilibrium.

As a model for a spherically symmetric star cluster, Henon [19] studied a system of concentric spherical mass shells. Each shell represents a collection of stars with the same radius and radial velocity. The stars move on the surface of the shell with the same magnitude of tangential velocity but in different directions. The magnitude of angular momentum is the same for all stars on a single shell; therefore, the radial motion of each star is governed by the same equation of motion. This allows the radial motion of all the stars on a shell to be followed by numerically integrating a single equation of motion. Angular momentum is conserved for each star, and since the radial motion of the shell is the same as that of one of its constituent stars, the singularity at the origin is shielded by the centripetal force. Henon found an initial collapse of the system of 1000 shells and a final state in a core halo configuration. A later study of a similar system by Yangurazova and Bisnotavyi-Kogan found similar results [21]; however, instead of integrating the equations of motion, the system was followed by determining the times at which the shells intersect. This resulted in a more accurate and efficient simulation for the following reasons: computer roundoff error was introduced only at intersections, the truncation error that is introduced by numerical integration methods was avoided, and less computer time was required to simulate the system.

In the studies of Refs. [19] and [21], an evolution to a core-halo configuration is exhibited. Both systems shield the singularity at the origin by the conservation of angular momentum, which avoids the gravothermal catastrophe described by Lynden-Bell and Wood. Here we describe our study of phase transitions in a similar system of concentric spherical mass shells, with the difference that the shells have zero tangential velocity. With no angular momentum, the origin will not be shielded, and a gravothermal catastrophe could occur. In order to investigate the existence of a phase transition, we shield the singularity by introducing an inner barrier with which the shells can collide elastically. This allows us to investigate the thermodynamic behavior of the system as the singularity at the origin is approached, by decreasing the radius of the inner barrier.

An initial study of this system explored the phase space of the two shell system to determine its ergodic properties, and compared it with the system of planar, parallel, mass sheets [22]. Reidl and Miller determined that the parallel sheet system with populations of ten or less has at least one stable periodic orbit, ruling out ergodicity [23]. Froeschle and Scheidecker [14] found that in a system with three mass sheets, only 4% of the phase space was actually occupied by chaotic orbits. In the system composed of two spherical shells, a much larger chaotic component was found when the energy of the system was above the threshold energy (where the fixed point of the system went from elliptic to hyperbolic), suggesting that the spherical shell system may reach equilibrium more quickly than the sheet system [22]. This was supported by a study by Youngkins and Miller [24], in which a system consisting of concentric spherical shells reached equilibrium on a time scale almost two orders of magnitude smaller than the sheet system. This suggests that the spherical shell system may be a more useful model for testing astrophysical theories concerning the evolution of stellar systems.

In the present work we extend our study of the spherical shell system to investigate the existence and behavior of phase transitions, both theoretically and via dynamical simulation. We consider three types of interaction with the environment: microcanonical (system is isolated from its environment), canonical (system is in contact with a constant temperature reservoir), and grand canonical (system is in contact with a reservoir of constant temperature and chemical potential). An abbreviated version of our preliminary results appeared earlier [25].

We first focus on the predictions of the mean field theory. We constrain the system to a spherical box, and shield the origin with a reflecting barrier. We find that in all three ensembles, there is a critical value of the inner barrier radius below which two phases are possible. The density profile for each phase is smooth, but one phase has a higher central concentration of mass. In the microcanonical ensemble, the more uniform distribution is the thermodynamically stable solution for higher energies, and the concentrated phase is stable at lower energies. The two solutions coexist at the transition point. A plot of the maximum entropy versus energy has a discontinuous slope at the coexistence point, indicating a discontinuous change in the temperature, and the system undergoes a phase transition. Mean field theory predicts a similar transition for the canonical system; however, the transition results in a discontinuity in energy instead of temperature. Also, the critical point occurs at different values of the inner barrier radius for the two ensembles. These dif-

ferences emphasize that the two ensembles cannot be used interchangeably, as they can in normal matter in which the energy is an extensive parameter. In the grand canonical system, we study a special case where the average mass of the system is constant in order to be able to compare the results to the other two ensembles. In this case, no phase transition is predicted; the equilibrium grand potential varies smoothly. The concentrated phase is thermodynamically less stable for all values of temperature and inner barrier radius.

Phase transitions are predicted only for systems with infinite population [26]. It is well known that for finite systems, the jump in the order parameter is smoothed into a rounded transition, the center of which is shifted from the value at which the transition occurs in the infinite system. The rounding and shifting of the transition depends on the population of the system, N, as $N^{-\gamma}$ and $N^{-\lambda}$, respectively [26]. In the following, we show that this is supported by dynamical simulation, in which the number of particles is finite. In both the microcanonical and canonical systems phase transitions were observed, but the transition was rounded over a range of energies (temperatures), and shifted from the transition point predicted by mean field theory. By varying the number of particles in the simulation, we demonstrated that the simulation results for the transition were consistent with the rounding and shifting behavior predicted by finite size scaling. As predicted by mean field theory, the grand canonical system showed no signs of a transition to the more concentrated phase, even when the system was prepared in a highly condensed configuration.

In addition to testing the predictions of mean field theory, we used dynamical simulation to study the behavior of fluctuations in the gravitating shell system. It is well known from critical phenomena [27] that long-range correlations in density fluctuations exist at the critical point. In normal matter, an attribute of systems that exhibit these correlations is a critical ''slowing down'' where the relaxation time diverges [28]. From dynamical simulation ($N=64$), we found that strong temporal and positional correlations do exist near and above the critical point; however, the relaxation time showed no sign of divergence at any point in the transition plane for the microcanonical (E,a) or the canonical ensemble (β,a).

In the following sections, we present our methodology for studying the spherical shell system, and the results obtained for the three ensembles in the mean field approximation and by dynamical simulation. Section II discusses the treatment of the system in the Vlasov (mean field) limit and a method for determining equilibrium density profiles, which are used to investigate the existence of phase transitions for the three ensembles. Section III describes the numerical simulation for the three different ensembles (microcanonical, canonical, and grand canonical), and in Sec. IV a comparison between the mean field approach and the simulation results is presented. In Sec. V, the behavior of correlations in the system are explored by dynamical simulation. Conclusions are presented in Sec. VI.

II. DENSITY PROFILES PREDICTED BY MEAN FIELD THEORY

For the shell system discussed in this paper, the exact calculation of the appropriate thermodynamic quantities (e.g., the density of states Ω or the partition function Z) proves intractable. Instead, as an approximation, we consider the system in the mean field limit of $N\rightarrow\infty$, while holding the total mass and energy constant. The shell system considered here is represented by a simple fluid flow in a two-dimensional $\mu(r,\nu)$ space with mass density $f(r,\nu,t)$. The evolution of the density function is given by

$$\frac{\partial f}{\partial t}+\nu_r\frac{\partial f}{\partial r}+\frac{d\nu_r}{dt}\frac{\partial f}{\partial \nu_r}=0. \tag{1}$$

There are an infinite number of stationary solutions $(\partial f/\partial t=0)$ to the Vlasov equation; here we are interested in the equilibrium stationary solution, the one which maximizes the entropy. The entropy extrema occurs when f is of the form [7]

$$f=Ae^{-\beta[(1/2)\nu^2-\varphi(r)]}=Ce^{-\beta\nu^2/2}\rho(r), \tag{2}$$

where A and C are normalization constants, $\beta=m/kT$, m is the mass of a single shell, k is Boltzmann's constant, T is the temperature and $\rho(r)$ is the linear mass density, $\varphi(r)$ is the gravitational potential, and

$$\varphi(r)=-GM\int_a^b dr'\,\rho(r')\left[\frac{\theta(r-r')}{r}+\frac{\theta(r'-r)}{r'}\right], \tag{3}$$

where $\theta(r-r')$ is the Heaviside unit step function and M is the total mass. In equilibrium, from Eqs. (1) and (2), the normalized linear mass density profile, $\rho(r)$ satisfies

$$\frac{d}{dr}\left[\frac{r^2}{\rho}\frac{d\rho}{dr}\right]=-MG\beta\rho(r), \tag{4}$$

subject to

$$\left.\frac{d}{dr}\rho(r)\right|_{r=a}=0 \tag{5}$$

and

$$\int_a^b\rho(r)dr=1, \tag{6}$$

where a and b are the radii of the inner and outer reflecting barriers, respectively. It is important to note that although similar in form, this system of equations for the mass density of the one-dimensional shell system is not the same as that for a spherically symmetric three-dimensional system: i.e., $\nu(r)$ is the radial velocity and $\rho(r)$ is the mass per unit length.

To solve for $\rho(r)$, Eq. (4) was decomposed into two first order differential equations in the variables $y_1=dy_2/dr$ and $y_2=MG\beta\rho$:

$$\frac{dy_1}{dr}-\frac{y_1^2}{y_2}+\frac{2y_1}{r}=\frac{-y_2^2}{r^2}, \tag{7}$$

$$\frac{dy_2}{dr}=y_1. \tag{8}$$

These equations were then integrated numerically using the Burlisch-Stoer numerical method [28].

Since only one boundary condition is specified [$y_1(a)=0$], we may arbitrarily choose the other boundary condition, $y_2(a)$ and solve the system of equations, yielding $y_2(r)$. From Eq. (6), integration of the function $y_2(r)$ from the inner to outer boundary yields $MG\beta$, and $\rho(r)$ (for the specified boundary condition) is then known explicitly. From $\rho(r)$, all thermodynamic functions of interest can be computed.

III. PHASE TRANSITIONS PREDICTED BY MEAN FIELD THEORY

Using mean field theory, we explored the microcanonical, canonical and grand canonical ensemble. In the microcanonical ensemble, the system is isolated from its environment. No exchange of energy or particles occurs at the outer barrier and the energy of the system is constant. For each solution of $\rho(r)$ for a given energy E, there is an associated entropy S:

$$S=-kN\left[2\beta E/M-\frac{1}{2}\ln\beta-\ln\rho(a)+\beta MG\int_a^b\frac{\rho(r)}{r}\,dr+\text{const}\right]. \tag{9}$$

Without loss of generality, we define units of distance, time, and mass for which $b=G=M$ (total mass)$=1$. Only the solution with the maximum entropy is stable, and hence is the equilibrium solution when it exists.

In the canonical ensemble, the system can exchange energy (but not particles) with a thermal bath. The average temperature of the system will remain constant. The free energy associated with each density profile, $\rho(r)$, is given by

$$F=E-TS=-E+\frac{M}{\beta}\left[\frac{1}{2}\ln\beta+\ln\rho(a)-\beta MG\int_a^b\frac{\rho(r)}{r}dr-\text{const}\right]. \tag{10}$$

In the canonical ensemble, the state with the minimum free energy is the equilibrium state [27]. In chemical systems where the energy is an extensive parameter, the microcanonical and canonical ensembles can be used interchangeably to explore macroscopic behavior [28]. However, in gravitational systems, where the energy is not extensive, this equivalence breaks down. One manifestation of this difference occurs in the heat capacity of gravitational systems. It is always positive for the canonical ensemble, but can become negative in the microcanonical ensemble near a phase transition [29].

In the grand canonical ensemble, the system can exchange both energy and particles with the thermal bath. The state with the minimum grand potential

$$\Phi=U-TS-\mu N=\frac{M}{\beta}[a\rho(a)-b\rho(b)] \tag{11}$$

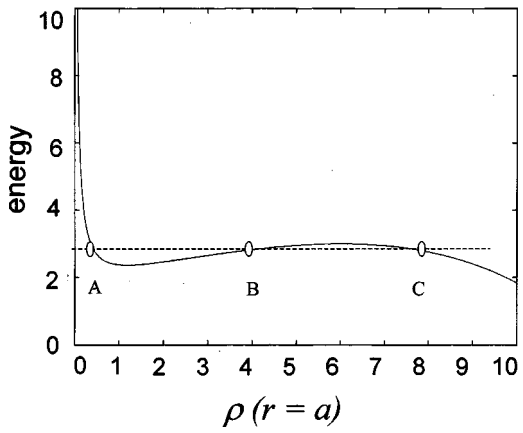

FIG. 1. Energy as a function of the density at the inner boundary for inner barrier radius, $a=0.001$. All units are dimensionless. The dotted line shows an energy value that has three corresponding density values (A, B, and C).

is the equilibrium state, where U is the potential energy of the system and μ is the chemical potential. We will demonstrate that the three ensembles lead to different results by examining the properties of phase transitions in all three ensembles.

In the microcanonical ensemble, for an inner barrier radius of say, $a=0.1$, there is a unique $\rho(r=a)$ for each energy. However, as the radius of the inner barrier is decreased below a certain threshold, there is a range of energies that admits three possible solutions (see Fig. 1). Figure 2 shows the corresponding density profiles for each of the three states. Both axes are logarithmic. The density profile of state A corresponds to the smallest density value at the inner barrier, and is almost uniform between the barriers. In contrast, state C has a density profile that corresponds to the largest density value at the inner barrier. Note that almost all of the mass is concentrated near the center of the system. State B has a density profile that lies between the two extremes of A and C. The amount of mass concentrated near the center of the system varies from state to state even though the energy for all three states is the same. To determine which state is the equilibrium distribution for a given ensemble, the appropriate thermodynamic quantity, e.g., entropy, free energy or grand potential, must be calculated.

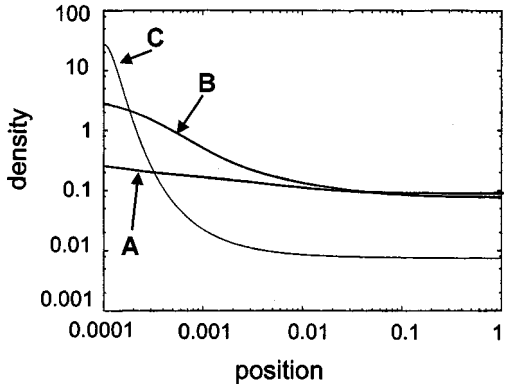

FIG. 2. Density profile for density points A, B, and C in Fig. 1. All units are dimensionless. State A corresponds to the smallest density value, C corresponds to the largest, and B lies between the two extremes (both axes are logarithmic).

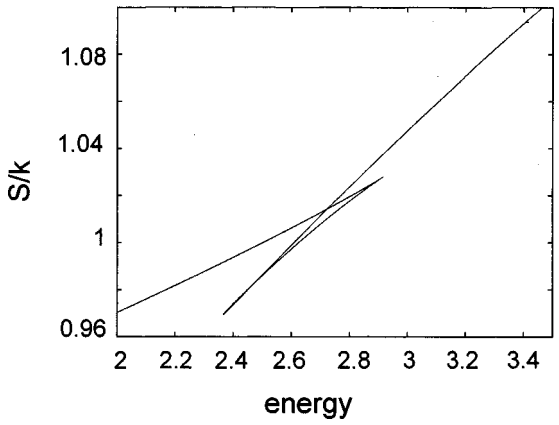

FIG. 3. Entropy vs energy for the microcanonical ensemble for all density profiles for inner barrier radius, $a=0.001$. All units are dimensionless. Note that there is a range of energies that has multiple entropy values.

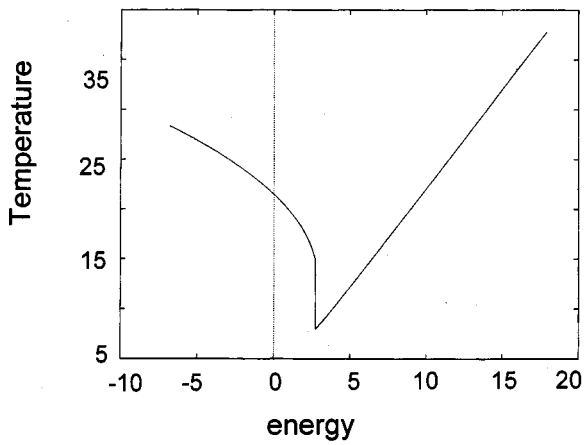

FIG. 4. Temperature vs energy for the microcanonical ensemble for system with an inner barrier radius, $a=0.001$. All units are dimensionless. The temperature changes discontinuously at $E=2.7$. Note that at energies below the transition point, the heat capacity (dE/dT) is negative.

For the microcanonical ensemble, plotting the entropy calculated for each of the states for an inner barrier radius $a=0.1$ (where the energy is single valued) yields a curve that is smooth with a one-to-one correspondence between entropy and energy; each point represents the maximum entropy state for a given energy. Since the slope of this line, $(\partial S/\partial E)_a = 1/T$, is continuous at all points, the temperature changes continuously, and no phase transition is expected at this value of inner barrier radius. As the inner barrier radius is decreased, however, this one-to-one correspondence vanishes, and there are a range of energy values that have three corresponding entropy values (see Fig. 3). The equilibrium curve has two branches, with a ''kink'' in the curve where the two branches intersect. The upper (higher energy) branch consists of solutions with density profiles which resemble that of state A shown in Fig. 2, with the mass almost evenly distributed between the barriers. The solutions on the lower branch have densities which resemble those of state C (Fig. 3) with most of the mass condensed at the center. At an energy value of 2.7 in our choice of units, the two branches intersect. At this point, two states with differing mass distributions (one roughly evenly distributed and one with a central condensation of mass) coexist. This coexistence differs from that at the phase transition point in chemical systems, where both phases can be physically present at the same time, e.g., the system consists of both liquid and vapor. For gravitational phase transitions this is not the case; the system can be in only one of the two possible states. The slope of the maximum entropy, β, changes discontinuously at the coexistence point signifying a first order gravitational phase transition with a discontinuity in temperature.

In common with chemical systems, each branch has solutions which continue past the transition point. This portion of the curve consists of metastable states, where the solutions are only locally stable. We will see in later sections that in the dynamical simulation, under certain conditions, these metastable states manifest themselves, and the average density profile of the simulation reflects that of the metastable state instead of the stable one. The portion of the curve which connects the two stable branches is thermodynamically unstable [28].

Figure 4 demonstrates how the temperature of the system changes as a function of energy. For high energies, the heat capacity is positive, as it is in normal systems with short-range forces. This positive heat capacity exists for energies down to $E=2.7$. At this point the temperature jumps to a higher value and as the energy decreases further, the heat capacity has a negative value.

A useful candidate for the order parameter of the system is the virial ratio, $VR=2T/|U|$, where T and U are the kinetic and potential energies of the system. A significant jump occurs in the virial ratio at the phase transition point, $E=2.7$ for the microcanonical system with inner barrier radius, $a=0.0001$. We will examine the behavior of the order parameter from simulation results in Sec. V to see how the time-averaged simulation results compare to mean-field theory (MFT).

The results shown above demonstrate the prediction of a phase transition in the mean field limit for an isoenergetic system with a specific inner barrier radius $a=0.001$. To more fully understand the existence of phase transitions, it is necessary to consider the full range of inner barrier radius values and determine which intervals produce phase transitions. To do so, we systematically calculated the maximum entropy curve for many inner barrier radius values, and determined if a kink occurred, and if so, the corresponding value of the energy. Figure 5 shows the results of this study in the phase plane (E,a). Above the critical point $a>0.00187$, the system did not experience a phase transition. Below the critical point, phase transitions occur and, as the inner barrier radius decreases, the transition energy increases.

Similarly, in the canonical ensemble, phase transitions are predicted by examining the minimum free energy curves. Figure 6 shows the free energy as a function of β when the inner barrier radius $a=0.001$. The equilibrium curve consists of two branches with different density profiles that meet at the transition point $\beta=0.018$. For low β values (high temperature), the density is quasiuniform between the inner and outer barriers; states with high β values have a mass concentration at the center.

Figure 7 shows how the temperature of the canonical sys-

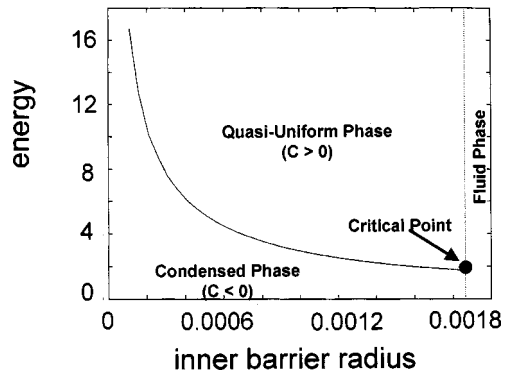

FIG. 5. Phase transition line for the microcanonical ensemble in the (E,a) plane. All units are dimensionless. The critical point lies at $a=0.00187$. The heat capacity C is negative for the condensed phase and positive for the quasiuniform phase. As the inner barrier radius decreases, the energy at which a transition occurs increases, suggesting that as the singularity at the origin is approached, more of the energy space is occupied by a negative heat capacity.

tem changes as a function of energy. This behavior is markedly different from the microcanoncial system (see Fig. 4), and demonstrates the breakdown of the equivalence in the microcanonical and canonical ensembles for gravitational systems. In the canonical system, the temperature changes continuously; it is the energy which exhibits a discontinuity. The reverse is true for the microcanonical system. Also, in the canonical system, the slope dT/dE is always positive, while the microcanonical system can exhibit negative specific heat once the inner barrier radius decreases below the transition threshold. It is interesting to note, however, that the values for the specific heat are significantly different on either side of the phase transition. At high energies, the temperature changes more rapidly for a given change in energy than occurs for lower energies below the transition point.

The mean field virial ratio was calculated for each state along the minimum free energy curve and plotted versus β. At $\beta=0.125$, the virial ratio jumps significantly. In Sec. V, we will examine the results of the dynamical simulations of the isothermal system with varying values of β to see if this transition occurs, and how its appearance is affected by the

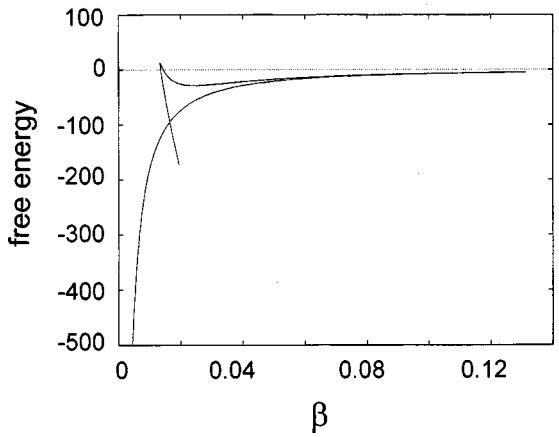

FIG. 6. Free energy vs β for the canonical ensemble for all density profiles for an inner barrier radius, $a=0.001$. All units are dimensionless. Between $\beta=0.015$ and 0.13, there is more than one free energy value for a given β.

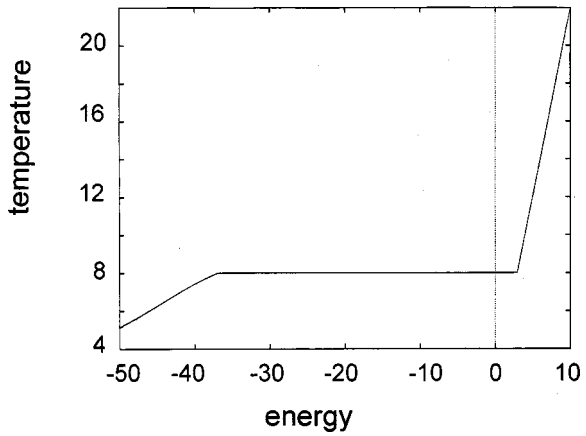

FIG. 7. Temperature vs energy for the canonical ensemble for the system with an inner barrier radius, $a=0.001$. All units are dimensionless. Note that there is no area of negative heat capacity that exists in the microcanonical ensemble. The energy changes discontinuously at $T=8$.

number of particles in the system.

The above results demonstrate that a phase transition occurs at one value of inner barrier radius for the isothermal system. We examined a range of inner barrier radius values, and determined the value of β at which a phase transition occurred, if one occurred at all. Figure 8 demonstrates the phase transition line in the β-a plane for the isothermal system. The critical point lies at $a=0.043$. Below the critical point, the transition temperature increases as the inner barrier radius decreases. This trend suggests that for an isothermal system with no shielding of the singularity, a phase transition would only occur at an infinitely high temperature.

In order to more easily compare the grand canonical ensemble with the others, we adjusted the chemical potential to maintain the total mass equal to unity. Similar to the entropy and free energy, the grand potential Φ exhibits a one-to-one correspondence with β for an inner barrier radius, $a=0.1$. However, as the radius of the inner barrier is decreased (Fig. 9), there exists a range of β that has two corresponding values of Φ. The minimum grand potential gives the equilibrium state; the lower portion of the curve is the stable solution. It is noteworthy that in the grand canonical case, unlike the other two ensembles, there is no discontinuity in the

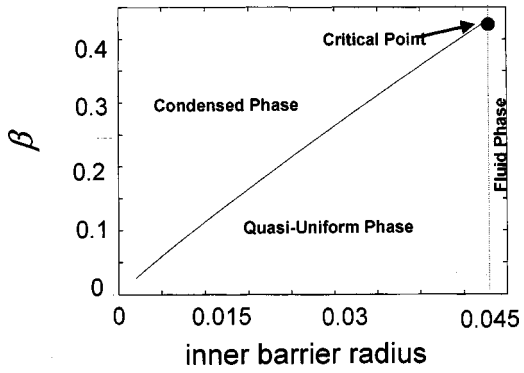

FIG. 8. Phase transition line for the canonical ensemble in the (β,a) plane. All units are dimensionless. The critical point lies at $a=0.043$. As the inner barrier decreases, the temperature at which a transition occurs increases.

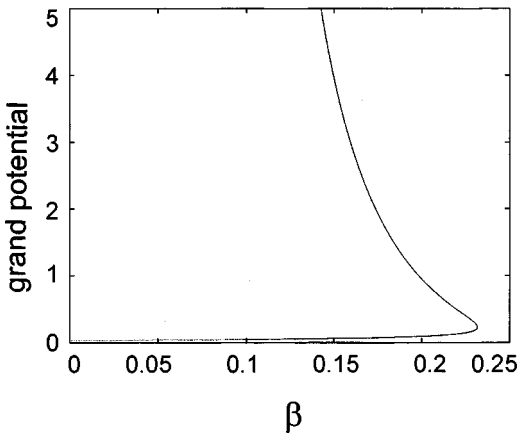

FIG. 9. Grand potential vs β for the grand canonical ensemble for an inner barrier radius, $a=0.01$. All units are dimensionless. Two different states exist for a range of β values; the minimum grand potential curve is the equilibrium solution. The slope of the equilibrium curve exhibits no discontinuity, so no phase transition occurs here. The chemical potential was adjusted to maintain a total mass of 1.

equilibrium curve, suggesting that no phase transition occurs in this ensemble. The density of this equilibrium phase is quasiuniform, resembling that of state *A* in Fig. 3. In Sec. V, we will show that these results are supported by a simulation in which both particles and energy can be exchanged with the environment.

IV. SYSTEM DESCRIPTION AND NUMERICAL SIMULATION METHOD

We considered a system of N concentric spherical mass shells of equal mass and uniform surface density. The shells move in a purely radial direction under their mutual gravitation and self-gravitation, with the acceleration of the ith shell given by

$$a_i = -Gm(i-\tfrac{1}{2})/r_i^2, \tag{12}$$

where the shells are numbered from innermost to outermost $i=1,2,\ldots,N$. This includes both the contribution from the interior mass and the self-acceleration of a given shell. G is the universal gravitational constant, m is the mass of an individual shell, and r_i is the radius of the ith shell. For the purposes of this study, we have chosen to use a system of units where $G=1$ and $m=1/N$ (the total mass of the system is equal to 1). The total energy of the system is conserved, and is given by

$$E=\sum_{i=1}^{N}\left[\frac{1}{2}\,m\nu_i^2 - Gm^2\left(i-\frac{1}{2}\right)\frac{1}{r_i}\right], \tag{13}$$

where ν_i is the velocity of the ith shell. The system is contained in a spherical box with reflecting boundaries. In addition, a reflecting inner barrier about the origin is added in order that we may study the influence of the singularity at the origin on the behavior of the system. Numerical difficulties prevent one from simulating a system where the radii of the shells decrease to exactly zero or to a very small value; the positions of the shells near the center become so close together that the finite precision of the computer prevents us from distinguishing the shells' positions, and their motion cannot be followed. However, by varying the radius of the inner barrier and allowing it to approach zero, we can gain insight into the singularity's influence. Similar shielding could have been obtained by imparting angular momentum to each shell, and a study of this rotational system is in progress by the present author (B.N.M.).

As the system evolves, the shells can intersect and pass through one another. When two shells cross, the amount of mass contained within each shell radius changes in a discontinuous manner, i.e., one shell's interior mass increases by $1/N$ while the other shell's interior mass decreases by $1/N$. This discontinuity in interior mass at a crossing gives rise to a discontinuity in each shell's acceleration and energy.

We have developed an algorithm that simulates the evolution of this system without numerically integrating the equations of motion. From the conservation of individual shell energy between crossings, it is possible to solve for the time that the ith shell will reach a specified radius r_i, given the initial time, $t_{0,i}$, the initial radius $r_{0,i}$, and shell energy E_i, by performing the integration

$$t_i - t_{0,i} = \pm\int_{0,i}^{r_i} dr\left[(2/m)\left(E_i+\frac{\alpha_i}{r}\right)\right]^{-1/2}, \tag{14}$$

where $\alpha_i=-Gm^2(i-1/2)$. The appropriate sign is given by the direction in which the shell is travelling, i.e., $(+)$ if the shell is moving away from the center, and $(-)$ if the motion is toward the center. The solution of the integral can take one of two forms, depending on the sign of the energy E_i.

The event driven algorithm used in this study is based on the ability to use the above equation to calculate the time a shell reaches a specific radius, given the shell's initial radius at an initial time and its individual energy. Three types of events are possible for a shell: collision with the boundary, turning point (only possible for a shell moving outward with negative energy), and intersection with another shell. Solving for the times of the first two types is straightforward; the radius of the event is known explicitly. The positions of the reflecting boundaries are fixed, and by setting a shell's velocity ν to zero in the equation for an individual shell's energy, the radius of the turning point can easily be calculated. However, the radius at which an intersection between two shells occurs cannot be determined analytically. Since the times at which the two shells reach an intersection are equal, we use a numerical method to solve

$$t_i(r_c, r_{0,i}, t_{0,i} E_i) = t_{i+1}(r_c, r_{0,i+1}, t_{0,i+1}, E_{i+1}), \tag{15}$$

for the crossing radius r_c, where t_i and t_{i+1} are given by the previous equation. In this study, a combination of bisection and the Newton-Raphson method, as described in the standard literature [30], was used to solve for the root of the above equation using a tolerance of 1×10^{-14}.

The basic strategy for the algorithm is to determine the times at which these events occur for all shells, and then sort these times to find the next event. The appropriate initial conditions are updated, and the process is repeated. This algorithm for following the evolution of the system has several advantages over one that numerically integrates the equa-

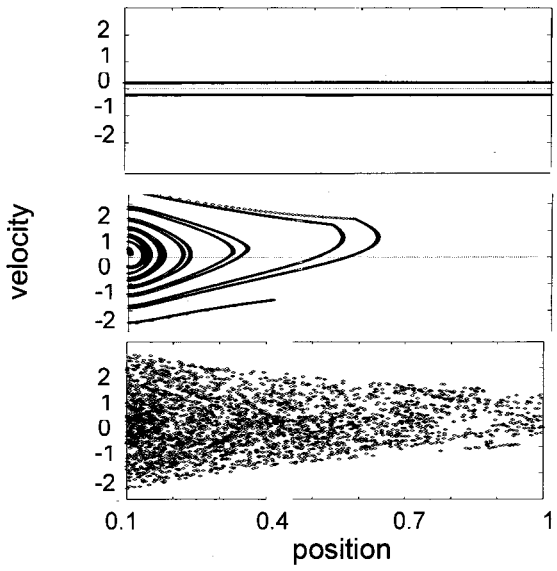

FIG. 10. μ space (position, velocity) for the $N=3200$ simulation at one time unit, 10 time units, and 14 time units. All units are dimensionless. Each shell's initial condition is represented by a point; the lines are due to the large number of particles and their proximity.

tions of motion. First the efficiency of solving only for event times allows the system to be followed for a much longer time. In addition, the truncation error associated with any numerical integration algorithm is avoided. Cumulative computer roundoff error is reduced, since error is introduced only at events instead of at every time increment, as is the case with numerical integration methods.

The action at the boundary can be varied in order to simulate different ensembles of statistical mechanics. For the microcanonical ensemble, the system is isolated and total system energy is conserved. In this type of simulation, collisions with the boundaries result in no change in the magnitude of velocity of the shell. For the canonical ensemble, the system is in thermal contact with a heat bath, and the average temperature is constant. To simulate this type of system, we use the outer barrier at $r=b$ as an isothermal wall for every hundredth collision. In such an event, detailed balance is respected by returning the shell to the system with a kinetic energy determined by randomly sampling the exponential distribution with mean T. In the grand canonical ensemble, the system can exchange both energy and particles with the bath. Dynamical simulation was accomplished by randomly introducing new shells at the outer boundary with a mean creation rate λ that is determined by the temperature and chemical potential of the reservoir we are simulating. To weaken the interaction with the virtual reservoir, the boundary was assumed to be ''semipermeable.'' To effect this, the creation rate was chosen to be one hundredth of the virtual external flux striking the outer barrier. The velocity of the newly introduced shell is determined by employing the same method as in the canonical case. To balance the flux of new particles entering at the boundary, every hundredth shell striking the outer barrier was removed from the system.

To assign initial conditions of a given energy, the shells are placed at equally spaced radii between the inner and outer barrier. This distribution determines the potential energy, and the total kinetic energy is calculated from the difference of the total energy and the potential energy. The total kinetic energy is then distributed equally among all particles with alternating signs of velocity. The first graph in Fig. 10 shows the μ space (position, velocity) for this configuration for a system of $N=3200$ shells. Due to the large number of particles and their close proximity, the individual particle symbols coalesce into a single line. In Sec. V we will discuss the behavior of systems with the same energy but with different initial conditions. These are selected by limiting the interval where the shells are initially placed, e.g., using only half of the region between the inner and outer barrier, resulting in different distributions of potential and kinetic energies for the system.

The second and third graphs in Fig. 10 show the evolution of the system at 10 and 14 time units. A convenient measure of time is a crossing time t_c, which is the time it takes a particle with no kinetic energy at the outer barrier to fall inward to the origin. t_c is approximately two of our dimensionless time units for the system of spherical shells discussed in this paper. The spiral behavior shown in the second graph can easily be understood. If there were no gravitational potential in the system, the shells would travel back and forth between the boundaries with a constant velocity. The time that it would take a given shell to traverse the system would not change regardless of the shell's relative position, i.e., how many shells are located inside its radius. Since the shells are initialized with the same magnitude of velocity, they would all have the same period, and they would all be in phase. Once the gravitational potential is considered, however, even shells that are near to one another will have different accelerations, causing their periods to vary, and they become out of phase with one another. This effect, known as phase mixing [3], causes the stream of particles to wind into a tight spiral pattern, which continues until the particles lose memory of their initial distribution.

In Sec. III, we demonstrated a method for calculating the density of the system as a function of radius in the mean field approximation of an infinite number of particles for a given energy and inner barrier radius. To compare MFT with the results of the simulation, we divided the interval between the inner and outer barriers into 20 cells of equal probability, i.e., the area under the mean field density curve is the same for each cell. The initial positions and velocities for the simulation were assigned according to the total energy and inner barrier radius specified for the mean field distribution. The system was sampled at equal time intervals (every $0.05t_c$), and the number of particles was accumulated in the appropriate cell according to the position of the shell. To determine when the density had reached its equilibrium distribution, a comparison was made between the current cell population and the cell population at half the current number of samples. Dividing each by the total number of samples normalized all cell populations. During a sample, $P_i=P_i(t)$ is the current time-averaged (normalized) population of cell i, and P_i' is the time-averaged (normalized) population of cell i at half the current number of samples, i.e., $P_i'=P_i(t/2)$. The simulation was stopped when the sum of the square of deviations between the time-averaged current population and the midtime population,

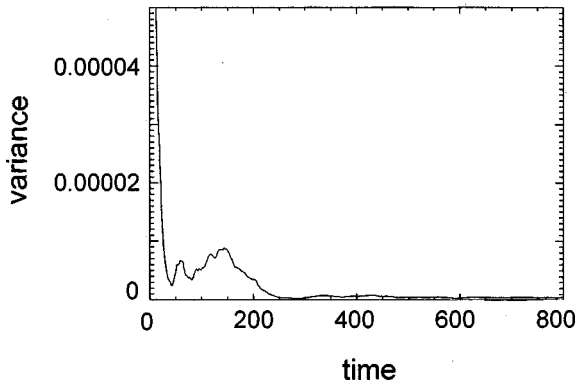

FIG. 11. The variance between the simulation (64 particles; the total energy is -0.8 and the inner barrier radius is 0.1) and MFT prediction is plotted vs time. All units are dimensionless. Note that in 800 time units, the fluctuations in variance have died out, and the system has relaxed.

$$\sigma^2=\sum_{i=1}^{20}[P_i-P_i']^2/20, \tag{16}$$

fell below 1.0×10^{-8}. The criteria we chose for terminating the simulation guarantees that we are well past the point where the system has settled down, and thus provides an upper bound for any reasonable choice of relaxation time. In Fig. 11, we replace P_i' with 1, the predicted mean field result, and plot the variance as a function of time for a 64-particle simulation. It is apparent from the figure that the fluctuations gradually vanish, indicating the approach to equilibrium. It is important to note that the variance settles down to some finite, nonzero value. This is due to the difference in density profiles, albeit small, between MFT and a simulation of a system with $N=64$.

V. COMPARISON OF NUMERICAL SIMULATION AND MEAN FIELD THEORY

Over the past few decades, several studies have predicted the occurrence of phase transitions in gravitating systems by using MFT to study the thermodynamic equilibrium state for various gravitational models [2,8,9,29], as we did for the system of concentric mass shells in Sec. III. However, until now, these predictions have not been verified by the dynamical evolution of the systems under consideration. Moreover, in order to include the hard-sphere interaction in a Vlasov mean field theory, they all employed some additional, *ad hoc*, assumptions. We have demonstrated the occurrence of a gravitational phase transition by numerically simulating a system of spherical, concentric, mass shells which move under their mutual gravitational interaction. The three ensembles of statistical mechanics that were examined in the mean field limit in Sec. III were simulated by varying the interaction of the system with its environment (see Sec. IV). In Sec. III, we showed that phase transitions were predicted by MFT for both microcanonical and canonical systems. In the grand canonical ensemble, multiple states existed for a given range of temperature; however, the equilibrium solution showed no phase transition, under the constraint of constant mean mass. Here we discuss the results of the numerical simulations for the three ensembles and compare them to the predictions of MFT.

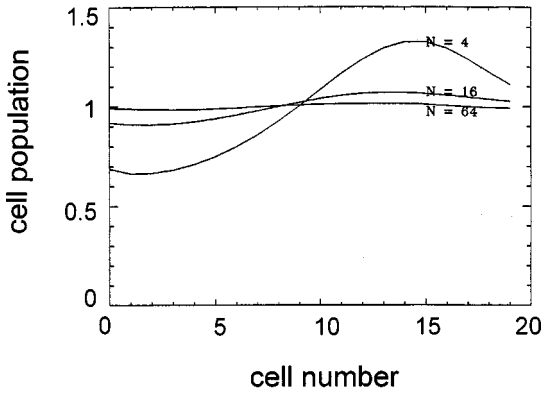

FIG. 12. The average density distribution for the simulation of the microcanonical system with four, 16, and 64 particles. All units are dimensionless. The mean field density is represented by a horizonal line at cell population of 1. The mean field limit is approached as the population increases, with excellent agreement for 64 particles.

Figure 12 shows the equilibrium density of the simulated microcanonical system for an inner barrier radius $a=0.1$ well above the critical value. The results for system populations of $N=4$, 16, and 64 are shown. The equilibrium density is determined by sampling the system at equal time intervals and determining, by its position, which cell each particle occupies (see Sec. IV). When the simulation has reached equilibrium, the population of the cells are normalized so that a cell population of unity corresponds to the mean field density distribution. Thus, compared with the MFT prediction, the distribution for the four-particle system shows a marked population deficiency in the inner cells and a surplus in the outer cells. The 16-particle case shows a similar structure, but the difference is smaller. For 64 particles, the density distribution shows excellent agreement with the MFT prediction. It is remarkable that a system with only 64 particles can so closely approximate a system with an infinite population.

The relaxation time for the shell system is much shorter than that found in the system of parallel mass sheets studied by Reidl and Miller [32]. Figure 11 shows the variance between the $N=64$ simulation and the mean field distribution as the simulation is carried out. By 800 time units, the fluctuations in variance have died out and the system has relaxed. Close examination of Fig. 11 shows a small residual difference between the simulation and MFT results even after the simulation has relaxed (4.3×10^{-7}). This residual difference increases with decreasing population with values of 3.6×10^{-3} and 4.1×10^{-2} for $N=16$ and 4, respectively. This is as expected, since the MFT distribution reflects an infinite population.

To investigate whether the system retains memory of its initial condition (which would suggest that equilibrium has not been reached), we created three different initial conditions for the same energy and inner boundary radius, with initial virial ratios varying between 0.06 and 1.3. All three cases (four, 16, and 64 particles) were run with the new initial conditions and the systems converged to final average

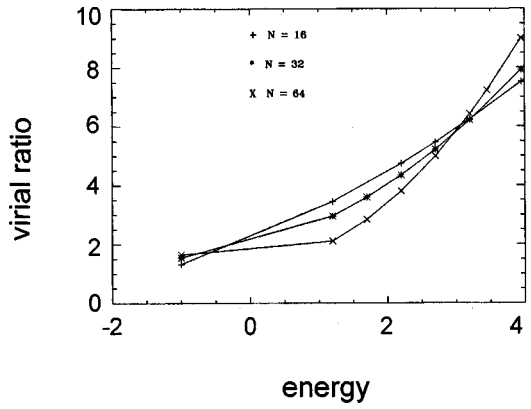

FIG. 13. Virial ratio vs energy for the transition region of the microcanonical system for $N=16$, 32, and 64. All units are dimensionless. The predicted transition point from the MFT is $E=2.7$. Note that the rounding and shifting of the transition decreases with increasing population.

density distributions which were nearly identical to the ones shown in Fig. 12.

The same study was performed for the canonical system above the critical point, $a>a_c$, and the grand canonical system above the point where two states exist, $a>a_2$ (recall the grand canonical ensemble, under the constraint of constant mean mass, does not exhibit a phase transition and thus will not have a critical point). Almost identical results were found for both ensembles. At 64 particles, the system approached the MFT distribution. In addition, for a given temperature and inner barrier radius, when the initial virial ratio was varied, the system relaxed to the same final density distribution. All three ensembles exhibited very similar behavior when the system was not in a region where multiple states exist for a given energy or temperature, and good agreement with MFT was achieved for a population of $N=64$ with variances on the order of 10^{-7}.

As the phase transition region is approached, however, differences between MFT and the simulation arise. It is well known that a system will exhibit a sharp transition only in the limit as $N\rightarrow\infty$ [26]. Finite size scaling theory predicts that systems with a finite number of particles will demonstrate a transition that is rounded and shifted compared to the MFT prediction [26]. The amount of rounding and shifting depends on the number of particles in the system, with the effect decreasing with increasing population. The range of energies over which the transition is broadened is given by

$$\Delta E = C_\gamma N^{-\gamma}, \tag{17}$$

where N is the number of particles in the system, C_γ is a proportionality constant, and γ is the rounding exponent. Similarly, the center of this rounding region is shifted from the location of the MFT transition by the relationship

$$E_c(N) - E_c(\infty) = C_\lambda N^{-\lambda}. \tag{18}$$

Figure 13 shows the equilibrium virial ratios for the microcanonical system in the transition region for systems with 16, 32, and 64 particles. The MFT transition occurs at $E=2.7$. As expected, the $N=16$ case shows the greatest rounding and shifting, which decreases as the population is increased to $N=64$. Using linear regression, we calculated the rounding and shifting exponents to be 0.97 and 0.74, respectively, with a goodness of fit of 0.98 and 0.99. The canonical system showed similar results. When compared with the MFT prediction, the results again agree; however, the values for the shifting and rounding exponents are different from the microcanonical case: 1.1 and 1.4, respectively.

Mean field theory does not predict a phase transition for the grand canonical case. There is a range of temperatures where both the concentrated state and the quasiuniform state exist, however, the quasiuniform state is the thermodynamically stable solution for all temperatures. To test if simulation bears this out, we conducted simulations in which the initial configurations were varied. Some had highly concentrated distributions of mass; others were more uniform. All cases converged to the quasiuniform state, as predicted by MFT. This stability of the quasiuniform state, as predicted by MFT and validated by simulation, is a further demonstration of the distinction between ensembles in systems with long range forces.

To test the robustness of the transitions, we started the simulations with both a concentrated and uniform distribution. The system almost always adhered to the predictions of MFT and evolved to the thermodynamically stable state, regardless of initial state. An interesting exception occurs in the canonical simulations for temperatures above the transition temperature. For systems with $N>16$, if the simulation was begun with the system in the concentrated phase, we did not observe a transition to the more uniform (and thermodynamically stable) phase during the typical run time of the numerical experiments. We believe this is a manifestation of the metastable state described in Sec. III. Posch, Narnhofer, and Thirring [31] found a similar phenomenon in a simulation of a two-dimensional system with an attractive force in contact with a thermal reservoir. When their system ($N=132$) was started in a uniform state with the temperature of the reservoir below that at which a transition to a concentrated phase should have occurred, the system did not collapse. In contrast to the concentrated metastable state demonstrated in the shell system for $N>16$, the two-dimensional cell system demonstrated a uniform metastable state. The authors of Ref. [31] did not study whether the existence of the metastable state depended on the number of particles in the simulation. For the shell system discussed here, however, the metastable state was not observed for the system with population $N>16$.

VI. RANGE OF CORRELATIONS

Developments in statistical physics have demonstrated an intimate connection between the onset of a phase transition and the size and evolution of fluctuations [26]. In turn, the behavior of fluctuations at the microscopic level is mirrored in the space and time dependence of correlation functions. These connections were rigorously established for the two-dimensional Ising model some time ago, and are experimentally manifested in the phenomena of critical opalescence. In particular, we know that near a thermodynamic critical point fluctuations evolve slowly and grow in size. From the standpoint of theory, both the relaxation time and the two body correlation length diverge there. However, the fact that a

phase transition cannot occur at finite temperature in a one-dimensional ''chemical'' system should prepare us for further unusual behavior in this investigation.

In analogy with chemical systems, it is natural to expect that near the gravitational critical point described in the preceding sections the persistence of large fluctuations would induce a marked increase in the time required for the system to equilibrate. The methodology we employed for determining the relaxation time was described in Sec. IV. When the variance between the time-averaged density computed both at times t and $t/2$ fell below 10^{-8}, the system was considered relaxed. In all simulations we found little difference in the relaxation time, suggesting the absence of critical point ''slow down'' and indicating that the behavior of fluctuations in systems with long-range interactions may differ significantly from their chemical counterparts.

In addition to exploring the predictions of mean field theory (which has nothing to say about fluctuations), dynamical simulation allowed us to compute both spatial and temporal correlation directly. By varying the inner barrier radius we were able to determine the influence on correlation of the singularity in the gravitational force in this one-dimensional system. Here we describe our studies of the decay of fluctuations of the total system kinetic energy, and the extent of spatial correlation of density fluctuations. We will see that the central features of the correlation spectra differ both quantitatively and qualitatively from our usual expectations.

Figures 5 and 8 show the coexistence curves for the microcanonical and canonical ensemble, respectively. We wish to demonstrate how the range of correlations behaves at various points in these planes. Specifically, we selected points below the phase transition line, at the phase transition line, above the phase transition line, at the critical point, a_c, and in the ''fluid'' region $a>a_c$, and examined the correlations in kinetic energy as a function of time and correlations in density as a function of position.

A. Temporal correlations

We calculated the correlations in kinetic energy as a function of time for the microcanonical and canonical ensembles,

$$C(\tau)=\lim_{t'\to\infty}\frac{1}{t'}\sum_{t=1}^{t'}[E_{\mathrm{kin}}(t)-E_{\mathrm{kin}_0}][E_{\mathrm{kin}}(t+\tau)-E_{\mathrm{kin}_0}], \tag{19}$$

where $E_{\mathrm{kin}}(t)$ is the kinetic energy of the system at the specified time and E_{kin_0} is the mean kinetic energy at equilibrium. To construct $C(\tau)$ for each of the simulations, we stored the value of the kinetic energy of the system at equally spaced intervals Δt as the simulation was being carried out. After the system had relaxed and the run was terminated, we used Eq. (19) with $\tau=n\Delta t$, $n=1,2,3$, etc. It is important to note that τ cannot be on the order of the total time that the simulation was run, because the number of terms in the correlation function will be greatly reduced, e.g., if τ is chosen to be one-half the simulation time there will only be half as many terms in the correlation function, which could add misleading fluctuations. For this reason, we have limited the value of $\tau<100$ time units. This proves sufficient, as all of the correlation functions have died out before this time. As C approaches zero for large τ, the kinetic energies at t and $t+\tau$ become statistically independent.

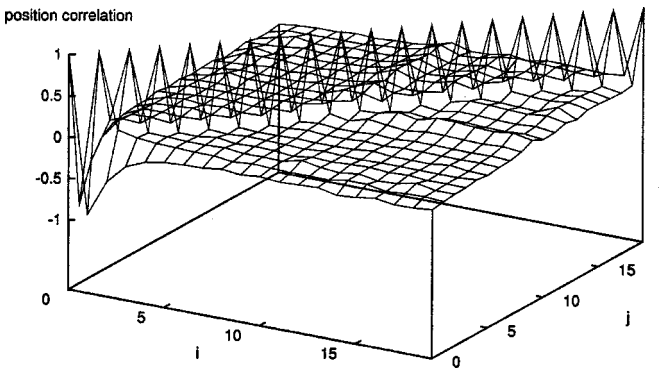

FIG. 14. Positional correlation function for canonical system below the transition line. Beta, $\beta=0.15$ and inner barrier radius, $a=0.01$. All units are dimensionless.

Striking differences are manifested between the two ensembles and within the ensembles themselves. The correlation function dies out much more rapidly for the canonical system than for the microcanonical system. It is likely that this is due to the temperature stabilization at the boundary in the isothermal system. Although the interaction is weakened by changing the velocity of the striking particle only every 100 collisions, the kinetic energy is driven to its equilibrium value more rapidly than in the case where no external mechanism exists to stabilize the temperature. Within the microcanonical system, the temporal correlations took longer to relax for the system in the fluid phase, $a>a_c$. In the canonical system, the system at the critical point and in the fluid phase exhibit this trend as well, although the differences between the cases are less marked. At and above the critical point, the correlation function has not relaxed at 25 time units, while below the critical point, all correlation functions have died out well before 25 time units.

B. Spatial correlation

The previous subsection demonstrates how the fluctuations in a single system parameter are correlated as the time between measurements is varied. Spatial correlations were investigated for this system as well, i.e., how regions of the system are correlated with respect to the distance between them. In Sec. IV, we described how the system was divided into 20 cells of equal probability, and how the population of each cell was recorded at each time interval to determine how the density of the system behaves over a long time scale. To determine the spatial extent of fluctuations in density, we calculated a correlation function between each pair of cells,

$$C_{ij}=\frac{1}{t'}\sum_{t=1}^{t'}[P_i(t)-\overline{P_i}][P_j(t)-\overline{P_j}]/\sigma_i\sigma_j, \tag{20}$$

where P_i and P_j are the populations of the cells i and j at time t and σ_i^2 and σ_j^2 are the variances of the population in cells i and j. Dividing by the variances normalizes the data so that self-correlation terms are equal to 1.

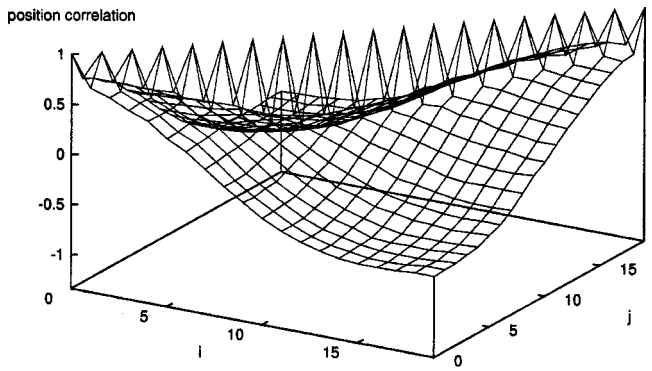

FIG. 15. Positional correlation function for canonical system at the critical point a_c. $\beta=0.425$, and the inner barrier radius $a=0.043$. All units are dimensionless.

The trends in positional correlation functions across the system are similar for both ensembles. For values of inner barrier radius less than the critical point, $a<a_c$, regardless of whether the system is above, at, or below the transition line, the correlations died out rapidly as the distance between cells increased (see Fig. 14). However, when the system is at the critical point, $a=a_c$, or in the ''fluid phase,'' $a>a_c$, strong correlations exist across the entire system (see Fig. 15). Examination of the value $C_{1,20}$ demonstrates the change in behavior for the system at the critical point and in the fluid phase. For values of $a<a_c$, $C_{1,20}$ is close to zero, $-0.1 \leqslant C_{1,20} \leqslant 0$. For $a \geqslant a_c$, the correlation function differs significantly from zero: $-0.78 \leqslant C_{1,20} \leqslant -.55$.

This change in behavior above the critical point is exhibited in both temporal and positional correlation functions, except for the kinetic energy correlation in the canonical system. We believe that this is due to the discontinuity in the velocity of the shells that collide with the temperature stabilizing barrier, which will drive the kinetic energy rapidly to its equilibrium value, and overwhelm any long-range correlations that exist in the system.

VII. CONCLUSIONS

The purpose of the present work was to explore the existence and behavior of phase transitions in systems with gravitational interactions. It is expected that the long range nature of these interactions will produce results different from those in ''normal'' systems, due to the nonextensive nature of the energy. In addition, this model probes the effects of the singularity of the gravitational force, which has been excluded from idealized models, such as that of Ref. [31]. To explore the behavior of the gravitational force, we studied a system of spherical, concentric mass shells, which move under their mutual and self gravitation. The study was pursued by two methods: (1) Theoretical: The system was considered in the mean field limit, where the number of particles in the system approaches infinity and the mass of each particle approaches zero. (2) Experimental: The dynamics of the system were simulated numerically on a computer. In the first method, only the equilibrium state is determined; no information about the approach to equilibrium is gained. In the second method, by simulating a finite number of particles, we were able to study the evolution of the system, and determine the effects of varying initial conditions of temperature and energy.

To study how interactions with the system's environment affected the behavior of phase transitions, we considered the system in three different ensembles of statistical mechanics: microcanonical, canonical, and grand canonical. In chemical systems, where the energy is an extensive parameter, these ensembles may be used interchangeably. However, one would expect that the long-range nature of the gravitational force would cause this correspondence to break down. We indeed find this to be true in both the mean field and simulation approaches; differences in the behavior of phase transitions between ensembles are significant. The results of MFT and simulation are summarized in Table I.

A. Microcanonical ensemble

The thermodynamic state is determined by the total energy E and the inner barrier radius a. Equilibrium states are states of maximum entropy $S=S(E,a)$. In the mean field limit, we found that below the critical point ($a<a_c$), for a certain range of energies, there were multiple states with the same value of energy E. Each of these states had a corresponding entropy S. For a given inner barrier radius below the critical point, plotting only the maximum entropy values for each energy, the entropy curve exhibits a ''kink.'' The change in slope for this line gives rise to a discontinuous jump in temperature signifying a phase transition. By definition, at the transition point two branches of the equilibrium curve meet. On the high energy branch, the density of the system is quasiuniform. Once the energy is lowered past the transition point, a more centrally concentrated phase exists. Plots of energy vs temperature demonstrate intervals in which the specific heat is negative.

We find similar results for the numerical simulation for the isoenergetic system. However, due to the finite number of particles in the simulation, the transition is no longer infinitely sharp. The transition line is rounded and shifted; this effect is more pronounced with decreasing population, and we determined a set of exponents that accurately described this behavior for the range of populations that were simulated in this study. It is noteworthy that the equilibrium distributions for the simulation were independent of the initial density distribution, and the final state always corresponded to the thermodynamically stable solution, regardless of the number of particles in the simulation. As we will see later in the discussion of the canonical ensemble, this is not always the case.

A study of temporal and positional correlation functions for the microcanonical simulations showed that in the fluid phase, long range correlations exist. Once below the critical point, regardless of the location in the (E,a) plane, the correlations quickly died out. One might expect that the long-range correlations near the critical point, $a=a_c$, might lead to a critical ''slowing down,'' i.e., the relaxation time would diverge; however, the relaxation time appeared to be independent of proximity to the critical point. It is important, however, to note that the maximum population for the simulations was $N=64$, and that increasing the population may better demonstrate the effect of correlations on the relaxation time.

TABLE I. Summary of mean field theory and simulation results.

	MFT				
	Ensemble				
	MCE	CE			
Critical point, ac	0.00187	0.0043			
Jump in virial ratio at transition pt.	3.3	7.2			
Jump in temp. at transition pt ($a=0.001$)	6.7	0			
Jump in energy at transition pt ($a=0.001$)	0	40.5			
$\rho(a)/\rho(b)$—collapsed	3820	3820			
$\rho(a)/\rho(b)$—intermediate	3.2	3.2			
$\rho(a)/\rho(b)$—quasiuniform	1.3	1.3			
	Simulation				
	MCE	CE			
Rounding exponent	0.74	1.14			
Shifting exponent	0.97	1.1			
MCE phase plane point	Transition pt	Above transition line	Below transition line	Critical point	Fluid phase
$C\ i=1,\ j=20$	−0.09	−0.08	0.03	−0.78	−0.55
Relaxation Time for E_{kin} corelation	45	70	65	80	90
CE phase plane point	Transition pt	Above transition line	Below transition line	Critical Point	Fluid phase
$C\ i=1,\ j=20$	−0.09	−0.1	−0.04	−0.57	−0.36
Relaxation Time for E_{kin} corelation	20	20	1	35	35

B. Canonical ensemble

In the canonical ensemble, the thermodynamic state is determined by the temperature T and the inner barrier radius a. Equilibrium states are states of minimum free energy $F=F(T,a)$. As in the microcanonical mean field limit, we found that below the critical point $a<a_c$, for a certain range of temperatures, there were multiple states with the same value of temperature. Each of these states has a corresponding free energy value F. A graph of the minimum free energies for each temperature exhibits a discontinuity in the slope in the equilibrium curve. The energy jumps at that point signifying a phase transition. At high temperatures, the density of the system is nearly uniform. At the transition point, both the uniform and a centrally concentrated phase exist, as they did in the microcanonical system. At temperatures lower than the transition point, the concentrated phase is the only stable solution. For all values of temperature, the specific heat is positive.

The numerical simulation for the isothermal system supports the predictions of the mean field approximation. Again, the transition is rounded and shifted due to the finite number of particles in the system. The exponents that describe the rounding and shifting were determined, and these accurately described the transition behavior for the range of populations that we studied. However, these exponents differed from those in the microcanonical system.

An interesting feature of the canonical system is the robustness of the concentrated phase above the transition temperature, where it is thermodynamically less stable. For systems with populations greater than $N=16$, if the system was initially concentrated, we were never able to observe a dynamical phase transition to the stable phase during the typical run times of the experiment. If the system was initially uniform in density, however, it always relaxed to the more stable solution, regardless of whether the stable state was concentrated or uniform.

The isothermal system demonstrated the same lack of critical ''slowing down'' as the isoenergetic system. Near the critical point, long-range correlations in time and position exist across the system; however, no significant difference in relaxation times occurred between any of the systems below, at, or above the critical point. In the isothermal system, the correlations in kinetic energy died out more rapidly than they did in the isoenergetic case, possibly due to the action at the outer wall, which works to thermostat the system.

C. Grand canonical ensemble

In the grand canonical ensemble, a thermodynamic state is defined by the temperature T and the chemical potential μ. Equilibrium states are states of minimum grand potential, $\Phi=\Phi(T,\mu,a)$. For the sake of comparison, for each T and a, the value of μ was fixed by requiring that the average system mass is 1, as it is in the microcanonical and canonical ensembles. Although there are values of temperature that have two states associated with it, plots of the minimum grand potential for each temperature do not exhibit the same kink, as demonstrated in the ensembles described above. The more uniform phase is predicted to be the more stable one over the entire (T,a) plane. Thus a transition to a more centrally condensed density profile is not predicted.

The results from the dynamical simulations were in complete accord with the mean field predictions. The system was

initiated with a variety of density distributions. In each case, the time averaged density profile agreed with that predicted for the more uniform profile. No sign of a transition was ever observed, even when the initial state was highly concentrated near the inner barrier.

SUMMARY

In this paper we have carefully studied the influence of the singularity of the gravitational potential on the system thermodynamics. We found that as the singularity is bared by decreasing the inner barrier radius, the system can exist in multiple phases. We investigated the nature of the transition in three different ensembles, and found significant differences between them. The difference between the canonical and microcanonical ensembles for this one-dimensional dynamical system had the same qualitative features as earlier mean field studies of three-dimensional systems in which the attractive singularity of the two-body potential was screened by a hard sphere interaction. However, our study of the grand canonical ensemble revealed unexpected results. To our knowledge, this is the first published investigation of an open gravitational system. The fact that the concentrated phase was never more stable in our study may have consequences for astrophysics for various stellar or even galaxy clusters which exchange both matter and energy with the environment, as well as planet formation in circumstellar disks. Our results suggest that further study over a wider range of mass, as well as in three dimensions, needs to be explored. In addition to the chief thermodynamic properties, our simulations also allowed us to investigate both spatial and temporal correlations in the system. In contrast with chemical systems, we found a remarkable picture of strong, system-wide, correlation throughout the fluid phase, and expected weak correlation in the multiphase region of the relevant thermodynamic state space for each ensemble.

[1] W. C. Saslaw, *Gravitational Physics of Stellar Systems and Galactic Systems* (Cambridge University Press, Cambridge, England, 1985).
[2] B. Stahl, M. K.-H. Kiessling, and Karl Schindler, Planet. Space Sci. **3**, 271 (1995).
[3] J. Binney and S. Tremaine, *Galactic Dynamics* (Princeton University Press, Princeton, 1987).
[4] H. C. Plummer, Mon. Not. R. Astron. Soc. **71**, 460 (1911).
[5] R. Emden, *Gaskugeln* (Teubner, Leipzig, 1907).
[6] V. A. Antonov, Vestn. Leningr. Univ. [Biol] **7**, 135 (1962).
[7] D. Lynden-Bell and R. Wood, Mon. Not. R. Astron. Soc. **138**, 495 (1968).
[8] P. Hertel and W. Thirring, Commun. Math. Phys. **24**, 22 (1971).
[9] E. B. Aronson and C. J. Hansen, Astrophys. J. **177**, 145 (1972).
[10] M. Kiessling, J. Stat. Phys. **55**, 203 (1989).
[11] J. Makino and M. Taiji, *Scientific Simulations with Special Purpose Computers: The GRAPE* (Wiley, Chichester, 1998).
[12] F. Hohl, Ph.D. dissertation, College of William and Mary, 1967 (unpublished).
[13] L. Cohen and M. Lecar, Bull. Astron. **3**, 213 (1968).
[14] C. Froeschle and J.-P. Scheidecker, Phys. Rev. A **12**, 2137 (1975).
[15] H. L. Wright, B. N. Miller, and W. E. Stein, Astrophys. Space Sci. **84**, 421 (1982).
[16] M. Luwel, G. Severne, and P. J. Rousseau, Astrophys. Space Sci. **100**, 261 (1984).
[17] J. H. Oort, Bull. Astron. Inst. Netherlands **6**, 289 (1932).
[18] M. Henon, Ann. Astrophys. **27**, 82 (1964).
[19] M. Henon, Mem. Soc. R. Sci. Liege (V) **15**, 243 (1967).
[20] M. Henon, Bull. Astron. **3**, 241 (1968).
[21] L. R. Yangurazova and G. S. Bisnovatyi-Kogan, Astrophys. Space Sci. **100**, 319 (1984).
[22] B. N. Miller and V. P. Youngkins, Chaos **7**, 187 (1997).
[23] C. J. Reidl, Jr. and B. N. Miller, Phys. Rev. E **48**, 4250 (1993).
[24] V. P. Youngkins and B. N. Miller, Phys. Rev. E **56**, R4963 (1997).
[25] Bruce N. Miller and Paige Youngkins, Phys. Rev. Lett. **81**, 4794 (1998).
[26] K. Binder, Ferroelectrics **73**, 43 (1987).
[27] D. Chandler, *Introduction to Modern Statistical Mechanics* (Oxford University Press, New York, 1987).
[28] L. E. Reichl, *A Modern Course in Statistical Physics* (Wiley, New York, 1998).
[29] T. Padmanabhan, Phys. Rep. **188**, 285 (1990).
[30] W. H. Press, S. A. Teukolsky, W. T. Vetterling, and B. P. Flannery, *Numerical Recipes in C* (Cambridge University Press, Cambridge, England, 1992).
[31] H. A. Posch, H. Narnhofer, and W. Thirring, Physica A **194**, 482 (1993).
[32] C. J. Reidl, Jr. and B. N. Miller, Astrophys. J. **318**, 248 (1987).